

# SINGLE-PHASE AND TWO-PHASE NATURAL CONVECTION IN THE McMASTER NUCLEAR REACTOR

A. S. Schneider and J. C. Luxat

Department of Engineering Physics, McMaster University,  
1280 Main St. West, Hamilton, ON , L8S 4L7, Canada  
[shneidas@mcmaster.ca](mailto:shneidas@mcmaster.ca) ; [luxatj@mcmaster.ca](mailto:luxatj@mcmaster.ca)

## ABSTRACT

A natural convection model has been developed for application to an open pool MTR facility at McMaster University. The model, adapted from a closed loop PWR model, is used for safety assessment of decay heat removal in the McMaster Nuclear Reactor under events that involve abnormal core cooling. The natural convection model calculates the steady state single or two-phase flow rate and quality rise along a fuel assembly given the inlet liquid pool temperature and assembly power. The model is constructed from first principles using the 1-D momentum conservation law, incorporating the Boussinesq approximation in the single-phase case and the Homogeneous Equilibrium Model assumptions in the two-phase case. It may also be useful for spent fuel pool treatments given appropriate adjustments. Unfortunately, to the authors' knowledge, there isn't enough applicable experimental work in the literature for comparison at this point, and validation of the model and the derived results will therefore not be discussed.

The safety evaluation combined the natural convection model with a lumped parameter model for evaluation of pool heatup and water vaporization to address various draining and pool boil off events. The approach was to calculate the steady-state natural convection flow rate developing in a fuel assembly and the resulting coolant and fuel temperatures for various pool (inlet) temperatures and assembly powers corresponding to the decay heat profile and slow pool heatup.

For all scenarios examined, clad and fuel temperatures remained well below limits associated with clad blistering or fuel melting. Consequently, natural convection and acceptable temperatures will be sustained in the McMaster Nuclear Reactor while the core remains covered. In the most severe draining examined, in which the pool drains to just before core uncover, it takes approximately a week (180 hours) after shutdown for boiling to start in the core.

## KEYWORDS

Natural Convection, Thermosiphoning, Material Testing Reactor, Research Reactor, Spent Fuel Pool

## 1. INTRODUCTION

A safety assessment for the McMaster Nuclear Reactor (MNR) has been carried out for postulated events associated with disruption of normal core flow and the establishment of Natural Convection (NC) flows in the reactor core. The MNR is a Material Testing Reactor (MTR) using MTR type fuel, currently operating at 3 MWt. The fuel assemblies consist of curved rectangular Low Enriched Uranium (LEU) fuel plates as is common in MTRs. Also, typical of MTRs, the MNR pool structure contains a number of beam tubes at mid-core level used for various neutron irradiation experiments. Normal operation entails downward gravity driven forced flow through the reactor core assemblies down to a holdup tank in which

$^{16}\text{N}$ , a product of irradiated oxygen in the water, can decay before the water is pumped back to the open reactor pool. Under conditions of low flow, a valve on the bottom of the pool, referred to as the “flapper”, opens naturally by reversal of pressure gradients, and creates a flow path back to the pool that enables the establishment of NC through the core within the reactor pool.

Events leading to the opening of the flapper are accompanied by reactor shutdown. The reactor automatic shutdown system initiates if low flow has been detected or if there is an indication that the flapper is open. Another reactor trip signal is generated on detection of low pool level. A scenario where the pump is shut down to mitigate a draining event will therefore also entail reactor shutdown. The most severe draining scenario is initiated by a break in one of the aforementioned beam tubes. This may, relatively quickly, lead to core uncover, and would at the very least cause some loss of pool inventory. The worst outcome of such draining will be partial uncover of the reactor core. In all scenarios which don't result in core uncover, it is expected that heat removal by NC will be the limiting heat transport mechanism, being less effective than forced flow. This will indeed be the case if the pump is shut down as a mitigating measure to limit the rate of pool draining or if a beam tube breaks causing the pump to flood and possibly short-out. With the intention of analyzing the spectrum of events before core uncover, this study investigated single and two-phase NC regimes under decay heat for different draining levels of the pool down to the top level of the core.

In the above scenarios, all parameters change very slowly, corresponding with accident conditions governed by the decay heat power profile. The fastest design basis draining scenario shows that draining to the core level would take at least 3.5 hours. Similarly, since the pool is very large, its heatup is slow even when it is isolated from the external heat sink (it takes more than 10 days to raise the pool temperature by 10 °C). The accident progression in the postulated scenarios is thus a slow process and it is therefore appropriate to examine the accident using a quasi steady-state model, taking steady-state ‘snapshots’ of the core and pool at different points on the timeline of the accident progression.

## 2. THEORY

### 2.1. Natural Convection Flow Loop

NC flow, or thermosiphoning, develops when warm fluid is picked up by natural buoyancy around a heat source. If the heat sink is above the heat source, the liquid cools at the heat sink, and is pulled back down by gravity if an alternate flow path from the heat sink back to the heat source exists. Such NC flow can be sustained purely due to gravity (and the heat source) as long as a flow path for the liquid to complete the loop exists. For an open pool this is sustainable at least as long as the pool level is above the core.

Zvirin [1] and Grief [2] both show that a common method for evaluating the flow characteristics of thermosiphons is by using the one-dimensional (1D) momentum conservation law integrated over the loop. Todreas and Kazimi describe a similar method applied on a Pressurized Water Reactor (PWR) in their textbook “Nuclear Systems” [3]. In their two-phase treatment they make use of the Homogeneous Equilibrium Model (HEM) which at first sight may appear inappropriate for use on MTR treatment because of the near atmospheric pressure conditions at which these reactors operate. However, Gambill and Bundy [4] have shown that for narrow rectangular channels typical to MTR fuel, usage of the HEM model is appropriate since vapor slip is substantially impeded in this geometry. Therefore, the treatment of Todreas and Kazimi is used as is, with adjustments of account for the MNR geometry and the open loop nature of the open pool.

The main adjustment is to focus on a single fuel assembly rather than on the entire core. This comes from the realization that the driving force for NC originates in each fuel assembly individually, governed by the assembly's own heat generation and hydraulic resistance, making the flow under this regime mainly an

individual assembly phenomenon. A loop treatment is then tailored to a MNR assembly as shown in Figs. 1a and 1b. The assembly is separated into sections according to the different geometric regions in it. The fuel meat within the plates is found vertically between points B and C as in Fig. 1 and does not fill section 4 entirely. The gap between the active fuel length and the plate edges is roughly 1 cm on each end. The exit and inlet are such that points A and F are on the same height, and so are D and E. The 1-D momentum conservation equation for single-phase flow in a channel parallel to the z axis is as in the book “Nuclear Systems” [3]:

$$\frac{\partial G}{\partial t} + \frac{\partial}{\partial l} \left( \frac{G^2}{\rho} \right) = - \frac{\partial p}{\partial l} - f \frac{G|G|}{2D\rho} - \rho g , \quad (1)$$

where  $G$  is the mass flux in  $\text{kg m}^{-2} \text{s}^{-1}$ ,  $\rho$  the density in  $\text{kg m}^{-3}$ ,  $p$  the thermodynamic pressure in Pa,  $f$  the friction factor and  $D$  the hydraulic diameter in m. Differentiation with respect to  $l$  signifies a path derivative. Eq. (1) is integrated along the loop in Fig. 1. For steady state, the time derivative term on the left hand side vanishes. The second term on the left hand side and first term on the right vanish after integration in the absence of a pump. The terms remaining after integration are:

$$\oint f \frac{G|G|}{2D\rho} dl + \sum_i K_i \frac{G|G|}{2\rho} = - \oint \phi \rho g dl . \quad (2)$$

It is appropriate to add the form losses as well to the total pressure loss if they are significant as has been done on the left hand side of Eq. (2) where  $K$  is the minor losses coefficient. Using the same notation as Todreas and Kazimi, the left hand side denoting the pressure losses is represented by  $\Delta p_f$  and the right hand side representing the driving pressure difference is represented as  $\Delta p_b$ . The driving term is essentially the pressure difference between the cold water column outside the assembly and the hotter water column inside it.

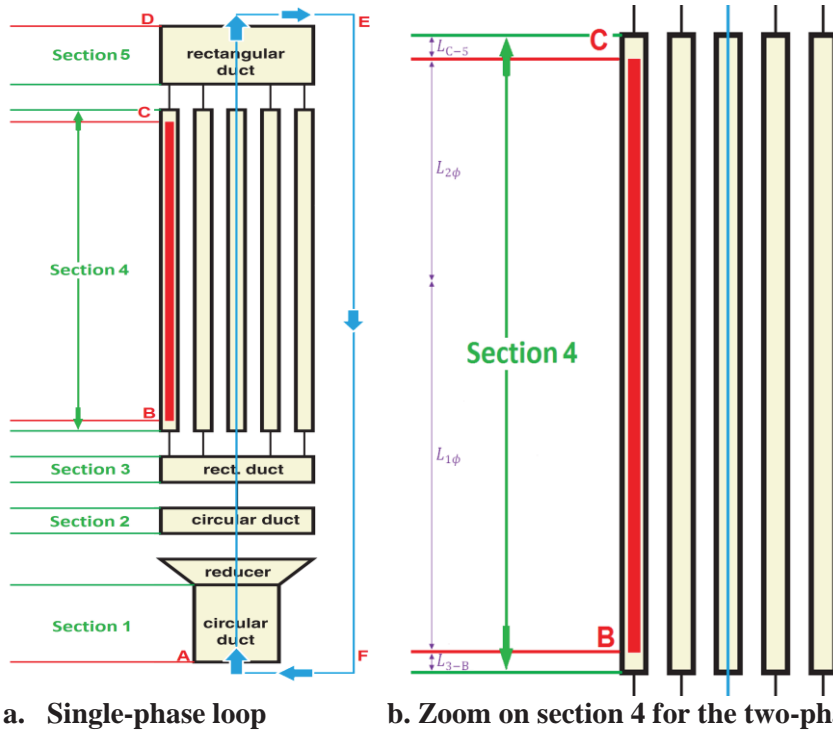


**Figure 1.** Representation of the flow loop through the MNR standard fuel assembly. (Source: MNR safety report).

### 2.1.1. Hydrostatic-buoyancy term in single phase

The driving term on the right hand side of Eq. (2) is integrated along the loop in Fig. 1. The integrals of the horizontal sections, from D to E and from F to A are equal to zero since there is no elevation change in them. The density from A to B is constant and equal to the ambient liquid density of the bulk pool water. The density change takes place from B to C. From C to D there is no density change but this new density is now lower, after being heated up between B and C. An assumption is made that due to the large body of water, the warm liquid dissipates to the bulk immediately after leaving the assembly at point D. Eq. (2) becomes:

$$\Delta p_b = -\rho_\infty g L_{AB} - \int_{Z_B}^{Z_C} \rho g dz - \rho_{out} g L_{CD} + \rho_\infty g L_{AD}, \quad (3)$$

where  $\rho_\infty$  is the density of the cold pool water,  $\rho_{out}$  the density of water after heating,  $L_{IJ}$  representing the length between any two points I and J and  $Z_I$  representing the height of point I above the bottom of the assembly. From geometry  $L_{EF} = L_{AD}$  and  $L_{AD} - L_{AB} = L_{BC} + L_{CD}$ , turning Eq. (3) into:

$$\Delta p_b = -\rho_\infty g (L_{BC} + L_{CD}) - \int_{Z_B}^{Z_C} \rho g dz - \rho_{out} g L_{CD}. \quad (4)$$

The axial heat flux shape in the reactor is that of a truncated cosine. It has been shown however, that the difference between performing the above calculation with the actual cosine shape and using a constant heat flux approximation is on the order of 5% [5]. Therefore, the integral from B to C is treated with linear assumptions. The heat flux is taken as a constant, giving a linear temperature rise along the heated section, i.e.  $\frac{dT}{dz} = const$ . Another assumption is that the change in density with temperature is also linear such that  $\frac{d\rho}{dT} = const$ . This comes from the Boussinesq approximation which will be addressed shortly. The density rise with height is therefore also linear, which solves the integral from B to C as:

$$\int_{Z_B}^{Z_C} \rho g dz = \frac{\rho_\infty + \rho_{out}}{2} g L_{BC} = \bar{\rho}_l g L_{BC}, \quad (5)$$

Inputting Eq. (5) into Eq. (4) gives:

$$\Delta p_b = (\rho_\infty - \rho_{out}) \left( \frac{L_{BC}}{2} + L_{CD} \right). \quad (6)$$

The Bousinnesq approximation for buoyancy driven flows is:

$$\rho(T) = \rho_\infty (1 - \beta(T - T_\infty)), \quad (7)$$

where  $T_\infty$  is the pool temperature and  $\beta$  is the thermal expansions coefficient in  $K^{-1}$ . Incorporating Eq. (7) into Eq. (6) gives:

$$\Delta p_b = \rho_\infty g \beta (T_{out} - T_\infty) \left( \frac{L_{BC}}{2} + L_{CD} \right), \quad (8)$$

where  $T_{out}$  is the exit temperature from the assembly.

Under steady state, the temperature rise along the assembly is given by:

$$T_{out} = T_\infty + \frac{\dot{Q}}{\dot{M}\bar{c}_p}, \quad (9)$$

where  $\dot{Q}$  is the assembly power in W,  $\dot{M}$  is the mass flow through the assembly in  $\text{kg s}^{-1}$  and  $\bar{c}_p$  is the average specific heat capacity along the heated channel in  $\text{J kg}^{-1} \text{K}^{-1}$ . A simplification is made by taking the length of  $L_{CD}$  as the length of section 5  $L_5$ , which is also conservative since  $L_5$  is slightly smaller than  $L_{CD}$ . Inputting Eq. (9) into Eq. (8) along with the above simplification gives:

$$\Delta p_b = \rho_\infty g \beta \frac{\dot{Q}}{\dot{M} \bar{c}_p} \left( \frac{L_{BC}}{2} + L_5 \right). \quad (10)$$

### 2.1.2. Losses term in single phase

The term on the left hand side of Eq. (2) represents the pressure losses along the loop. By incorporating the Boussinesq approximation, the density change is ignored in the losses term. The left hand side becomes:

$$\Delta p_f = \Delta p_{maj} + \Delta p_{min} = \sum_{i=1}^5 \frac{f_i L_i}{D_i} \frac{\rho_\infty v_i^2}{2} + \sum_{j=1}^6 K_j \frac{\rho_\infty v_j^2}{2}, \quad (11)$$

where  $\Delta p_{maj}$  is the major (friction) losses term and  $\Delta p_{min}$  is the minor (form) losses term. Index  $i$  is summed over the sections of the assembly and  $j$  is summed over the intersections of geometry changes in the assembly and the inlet and exit losses, where  $K$  is the minor losses coefficient. The conservation of mass for non-compressible flow is:

$$\dot{M} = \rho_\infty A_i v_i, \quad (12)$$

where  $A_i$  is the cross-sectional area of flow for section  $i$  and Eq. (11) is true for all sections. Inputting Eq. (12) into Eq. (11) gives:

$$\Delta p_f = \sum_{i=1}^5 \frac{f_i L_i}{D_i} \frac{\dot{M}^2}{2 \rho_\infty A_i^2} + \sum_{j=1}^6 K_j \frac{\dot{M}^2}{2 \rho_\infty A_j^2}. \quad (13)$$

The minor pressure loss between two geometries is defined conservatively by the higher flow velocity among them, which in Eq. (13) entails using the smaller cross-section area  $A_j$  between every two sections. The friction loss coefficients are found by use of the Colebrook-White correlation for turbulent flows and the laminar analytical Re number dependence for laminar flows [6]. The form coefficients are taken from literature for the given geometry and cross-sectional area changes. Both are adjusted by correction factors for rectangular channels in the rectangular sections.

### 2.1.3. Single-phase NC flow rate

By substituting Eq. (13) and (10) into Eq. (2) an expression for the steady state NC flow rate is found:

$$\dot{M} = \sqrt[3]{\frac{2 \beta g \rho_\infty^2 \dot{Q}_a (L_{BC}/2 + L_5)}{\bar{c}_p \left( \sum_i \frac{f_i L_i}{D_i A_i^2} + \sum_j \frac{K_j}{A_j^2} \right)}}. \quad (14)$$

Eq. (14) requires some iteration in order to be solved since the friction factors are dependent on the flow rate.

#### 2.1.4. Hydrostatic-buoyancy term in two phase

Similarly to the earlier approximation of taking  $L_{CD}$  as  $L_5$ , an additional major simplification is added by taking  $L_{BC}$  as  $L_4$ . The two are very close and since the clad is made out of highly conducting aluminum, using the heated channel's length as  $L_4$  isn't a major adjustment. An equivalent definition for the hydrostatic term presented in Eq. (3) is also given in "Nuclear Systems" [3]:

$$\Delta p_b = (\bar{\rho}_{\text{cold}} - \bar{\rho}_{\text{hot}})g(L_4 + L_5), \quad (15)$$

where  $\bar{\rho}_{\text{hot}}$  is the mean density in the heated section and the adjustment of  $L_{BC}$  has been incorporated within. Since immediate dissipation is assumed to the outside colder liquid, the cold leg mean density  $\bar{\rho}_{\text{cold}}$  is taken simply as  $\rho_\infty$ .

The void fraction's dependence on flow quality under HEM assumptions is:

$$\alpha = \frac{1}{1 + \frac{1-x\rho_g}{x \rho_f}}, \quad (16)$$

where  $\rho_g$  is saturated vapor density,  $\rho_f$  is saturated liquid density, and  $x$  is the flow quality. The two-phase mixture density is by definition:

$$\rho_m = \alpha \rho_g + (1 - \alpha) \rho_f. \quad (17)$$

Inputting Eq. (16) into Eq. (17) and rearranging:

$$\rho_m = \frac{\rho_f}{1+x(\rho_f/\rho_g-1)} \cong \frac{\rho_f}{1+x\rho_f/\rho_g}, \quad (18)$$

where the last transition is true for near atmospheric pressures where the liquid density is 3 orders of magnitude larger than that of the vapor density. The HEM model is similarly linear to the single-phase model used, in that all axially dependent parameters in the heated section are linear, provided the axial power distribution remains constant as before. The quality rise along the channel can then be expressed by:

$$\frac{dx}{dz} = \frac{x_{\text{out}}}{L_{2\phi}}, \quad (19)$$

where  $x_{\text{out}}$  is the exit quality and  $L_{2\phi}$  is the length of the channel occupied by the two-phase mixture as in Fig. 1b. It is also useful to define the following grouping of variables following Todreas and Kazimi:

$$\gamma \equiv x_{\text{out}} \frac{\rho_f}{\rho_g}. \quad (20)$$

The mean hot leg density can now be found:

$$\bar{\rho}_{\text{hot}} = \frac{1}{L_4 + L_5} \int_{Z_4}^{Z_D} \rho dz = \frac{1}{L_4 + L_5} \left( \bar{\rho}_l L_{1\phi} + \frac{\ln(1+\gamma)}{\gamma} \rho_f L_{2\phi} + \frac{1}{1+\gamma} \rho_f L_5 \right), \quad (21)$$

where  $Z_4$  is the height at start of section 4 and  $\bar{\rho}_l$  is again the average density in the single-phase portion. Substituting Eq. (21) into Eq. (15) produces the expression for the two-phase hydrostatic driving term.

### 2.1.5. Losses term in two phase

The difference in the pressure losses term in the two-phase case is the multiplying of two-phase regions by the two-phase multiplier. Otherwise the factors are the liquid only friction factors. The affected sections are the ones associated with the lengths  $L_{2\phi}$  and  $L_5$ . The two-phase multiplier in HEM is defined as:

$$\phi^2 = \frac{\rho_f}{\rho_m}. \quad (22)$$

The average two-phase multiplier for the length  $L_{2\phi}$  is therefore:

$$\bar{\phi}_4^2 = \frac{1}{L_{2\phi}} \int_{Z_f}^{Z_5} \frac{\rho_f}{\rho_m} dz = 1 + \frac{\gamma}{2}, \quad (23)$$

where  $Z_f$  is the height of liquid saturation and onset of the two-phase region. Similarly the average two-phase multiplier for section 5 is:

$$\bar{\phi}_5^2 = 1 + \gamma, \quad (24)$$

Terms in Eq. (13) are now multiplied by their appropriate multipliers in order to express the pressure losses for the two-phase case. The geometry changes from section 4 to 5 and the exit losses from section 5 are also multiplied by their local two-phase multiplier, which is equal to  $\bar{\phi}_5^2$ .

### 2.1.6. Two-phase NC flow rate

A couple of additional relations are needed in order to express all variables as functions of the flow rate. The exit quality is given by:

$$x_{out} = x_\infty + \frac{\dot{Q}}{\dot{M} h_{fg}}, \quad (25)$$

where  $x_\infty$  is the thermodynamic quality of the subcooled inlet and  $h_{fg}$  is the latent heat of vaporization in  $J kg^{-1}$ . This in turn gives  $\gamma$  as a function of  $\dot{M}$  as well. Also, since the enthalpy rise along the channel is considered linear the following relation can be obtained:

$$\frac{L_{1\phi}}{L_4} = \frac{0 - x_\infty}{x_{out} - x_\infty}, \quad (26)$$

and  $L_4 = L_{1\phi} + L_{2\phi}$ .

An expression for the flow rate can now be achieved by substituting Eq. (15) and the two-phase modified Eq. (13) into Eq. (2). The resulting transcendental equation is solved graphically for a given power and has, for certain powers, more than one solution.

## 2.2. Decay Heat Profile

To provide context, the pool time dependent heatup can be estimated to provide the time dependent inlet temperature for the core. In order to do so the decay heat profile is required. A classic correlation fitting with the ANS-5.1 standard for decay heat is given by El-Wakil [7]:

$$P = 0.095P_0 t^{-0.26}, \quad (27)$$

where  $P_0$  is the full power before shutdown in power units and  $t$  is the time after shutdown in seconds. The total energy emitted by the core from shutdown to time  $t$  is accordingly:

$$E = \int_0^t P(t') dt' = 0.128P_0 t^{0.74}. \quad (28)$$

The power figures for the core and the assembly are taken for an operating power of 5 MW which is the highest permitted by license plus a safety margin as used in the facility's safety report.

### 2.3. Pool Heatup and Vaporization

Again, in order to put the model into context and perform a number of estimations, a simplistic evaluation of pool heatup and vaporization (if saturation is reached) is performed. The energy emitted from the core is assumed to be fully absorbed by the pool water, and a conservative simplification is made by ignoring heat losses from the pool to the containment and structure. The time dependent temperature rise of the pool is therefore:

$$T_\infty = T_\infty(0) + \frac{E}{M_\infty \bar{c}_p}, \quad (29)$$

where  $M_\infty$  is the mass of the pool inventory in kg. Define the amount of energy deposited into the pool at a certain period of time  $t_1 < t < t_2$  by  $\Delta E = E(t_2) - E(t_1)$ , the height lost by vaporizing some of the pool's water in that period is:

$$\Delta H = \frac{\Delta E}{h_{fg} \rho_f A_{pool}}, \quad (30)$$

where  $A_{pool}$  is the pool's surface area in  $\text{m}^2$ . Eq. (30) neglects vapor buildup in the containment which would slow down the vaporization rate and both Eq. (29) and (30) neglect evaporation at all temperatures.

### 2.4. Heat Transfer Correlations

The heat transfer coefficients used to estimate the clad and fuel temperatures are the following. For laminar single-phase flow the heat transfer coefficient is the one resulting from the analytically obtained Nu number for rectangular channels [8]. For turbulent single-phase flows the classic Dittus-Boelter is used [9]. For two-phase heat transfer Kandlikar's correlation is used [10].

### 2.5. Clad and Fuel Temperatures

A relation between clad and fuel temperatures to the calculated coolant temperature is required. For thin long rectangular plates it is safe to assume that the heat flow is only in the direction perpendicular to the plate's surface. The resulting clad temperature at a given point is:

$$T_c = T_w + \frac{q''' w_{fm}/2}{h}, \quad (31)$$

where  $T_w$  is the water's temperature in  $^\circ\text{C}$ ,  $q'''$  the volumetric heat generation in units  $\text{W m}^{-3}$ ,  $w_{fm}$  the fuel meat thickness and  $h$  the heat transfer coefficient in  $\text{W K}^{-1} \text{m}^{-2}$ . The fuel centerline temperature is given by:

$$T_{fm} = T_c + q''' \left( \frac{w_{fm}^2}{8k_f} + \frac{w_c}{2k_c} \right), \quad (32)$$

where  $k_f$  and  $k_c$  are the fuel and clad thermal conductivities respectively in  $\text{W K}^{-1} \text{m}$  and  $w_c$  is the clad thickness.

### 3. RESULTS AND DISCUSSION

At the first stage after the onset of draining or other initiating events, single-phase NC will be established in the core channels until the temperatures in the channels start approaching saturation levels. Therefore, at this point, a figure of interest will be the amount of time it takes to reach saturation and onset of boiling in the channels. This is done for the spectrum of draining heights from full inventory to just before reaching core top. Another conservative simplification is made by performing calculations as though the draining was instant, having larger power figures and smaller inventories than in reality. A final conservative adjustment is made by calculating the temperature rise in the hottest channel by using the fraction of the calculated assembly flow for a single channel.

A full pool inventory scenario is presented in Fig. 2. The figure depicts the coolant's temperature profile with time at the exit from the hottest channel. Initially, the temperature trend is governed by the sharp drop in decay heat power, until the decay heat profile reaches the near plateau at around 1% full power. From that point on the temperature rise is governed by the slow rise in pool temperature until the simple model predicts pool saturation at 100 days. As seen in Fig. 2, the channel exit temperature doesn't reach saturation conditions even when the pool is at saturation, since the boiling is locally suppressed by the

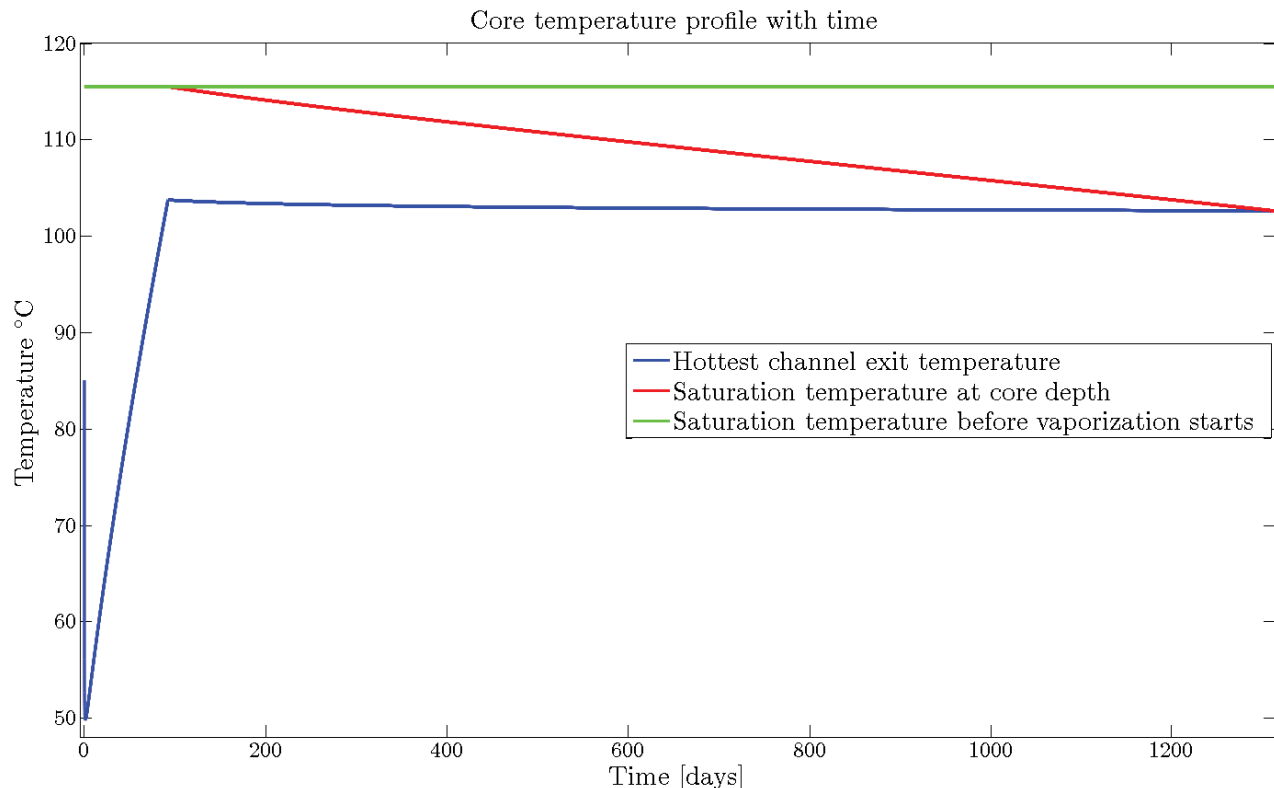


**Figure 2. Coolant temperature at hottest channel exit for full inventory.**

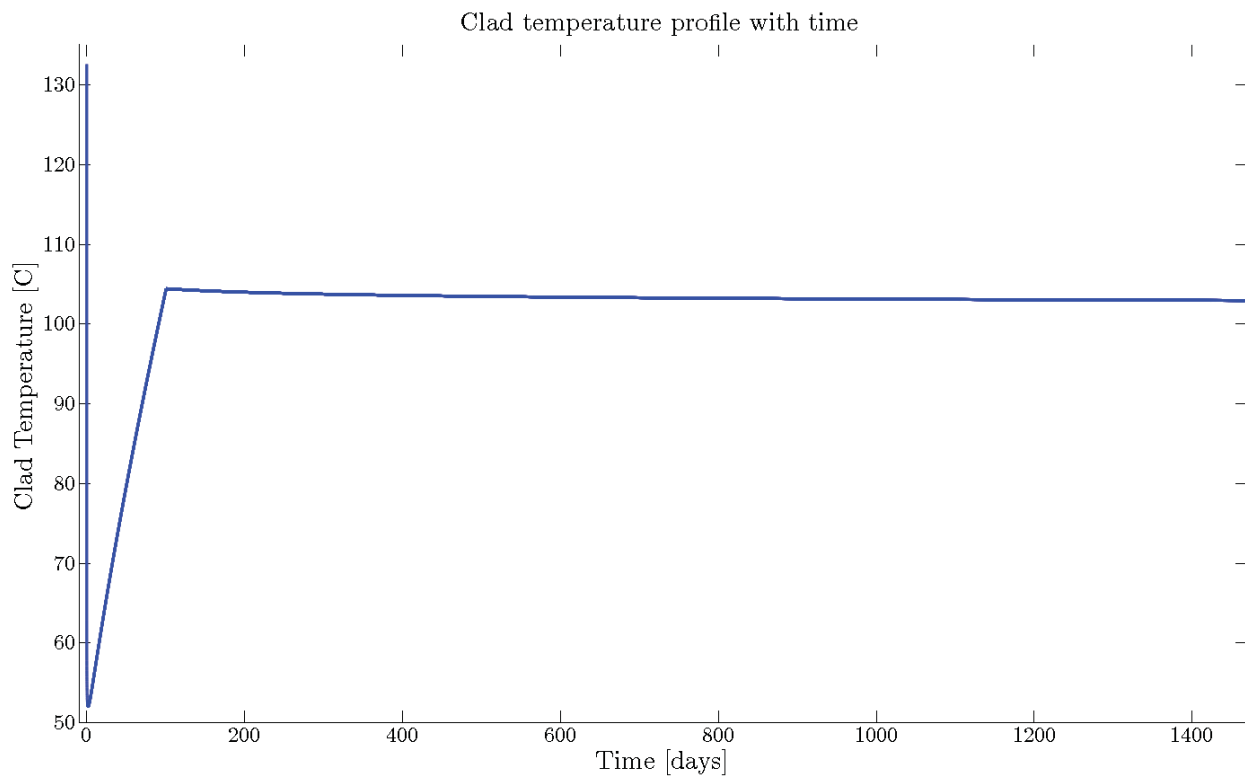


**Figure 3. Clad temperature at hottest channel exit for full inventory.**

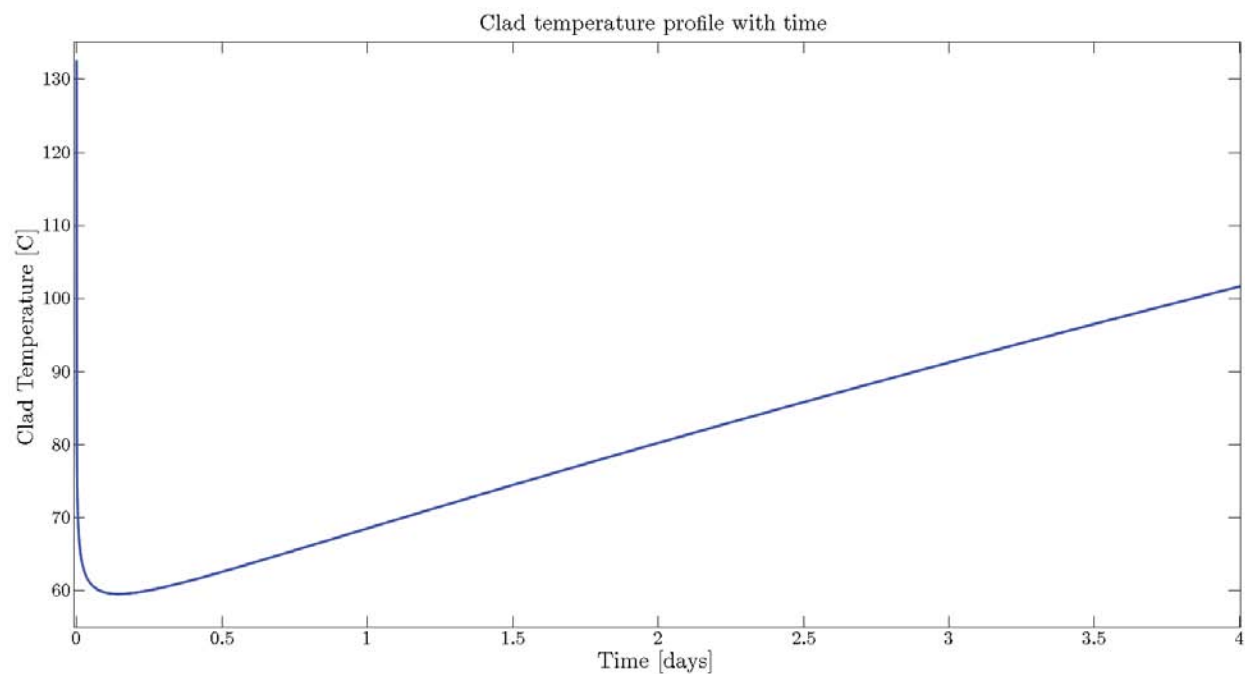


**Figure 4. Clad temperature at hottest channel exit for draining to core top.**

static head of water above the core. At this point the vaporization calculation starts and the saturation temperature at core depth starts slowly dropping as the column of water above the core slowly diminishes. The coolant exit temperature is also very slowly dropping from this point on, since the inlet water has reached its maximum saturation temperature and the power keeps dropping. Saturation at the hottest channel's exit won't occur until enough water has been vaporized to drop the pressure at the core exit level to the point where the exit temperature becomes the saturation temperature.

The corresponding clad temperatures to the two extremes examined are presented in Fig. 3 and 4 respectively. In both cases clad temperature is at all times much lower than any safety limit, starting from around 450 °C for blistering effects in aluminum. Since the plates are very thin, the fuel centerline temperature was found to be very close to clad temperature under all conditions.

At the other extreme, of draining the pool down to core top level, the hottest channel's exit temperature reaches saturation before the pool does, after about 7.5 days. The saturation temperature at core depth this time is the usual 100 °C at atmospheric pressure.

A summary of times for onset of boiling in the channels for various draining heights is presented in Fig 7. It can be seen that times of interest appear below the height of 1.81 m above the core, at which the model starts predicting boiling in the core before reaching pool saturation. At heights greater than 1.81m, boiling in the core channels is highly implausible.

The next stage after the onset of boiling is two-phase NC. A span of flow qualities at the exit of the assembly for different powers at nominal operation pool temperature (highest permitted) and full inventory is presented in Fig. 5. As can be seen, for high subcooling the two-phase model predicts a sharp step increase from no quality (assumed to represent single-phase liquid) to about 20% quality at a certain power. The point at which the slope of the quality profile starts rising is assumed as the onset of boiling for the two-phase model. As the subcooling decreases it becomes more difficult to establish this point as the slope becomes much more gradual, as can be seen in Fig. 6.

For the use of the two-phase model in the safety assessment, it was intended to continue the time evolution of the system as portrayed in Fig. 2 after the onset of boiling, by calculating the flow rates and subsequent temperatures through the latter. The parameters associated with the onset of boiling at the points presented in Fig. 7, the important of which being power, pool height and pool temperature, were inserted into the two-phase model in order to find the corresponding flow rates and exit qualities. The temperature calculation was performed conservatively as in the single-phase case using the hottest channel for the average flow rate.

It was found that for all conditions found in Fig 7. the two-phase model predicted that the liquid is still subcooled at the edge of the channel. In general this model mostly predicted the onset of boiling at higher powers than those predicted by the single-phase model. Therefore, the flow rate and temperatures were calculated for higher powers, the lowest at which the two-phase model predicted boiling. Using the above, the highest estimated clad temperature for all scenarios in Fig. 7 was 109 °C, as seen from the second series in the figure. The time dependent calculation was deemed unnecessary to be continued after this point for a few reasons. First, the power keeps on dropping with time while the two-phase model doesn't predict the onset of boiling even for the conditions presented at Table I. Second, since the two-phase convective heat transfer is much larger than the single-phase convection, it is expected, that the clad temperatures will remain relatively close to coolant saturation temperatures for qualities below those corresponding to Critical Heat Flux (CHF), and significantly below 450 °C. As mentioned by Gambill and Bundy, CHF is expected for combinations of high vapor qualities with larger power densities [4], both much larger than those expected in MNR normal operation and decay heat power.

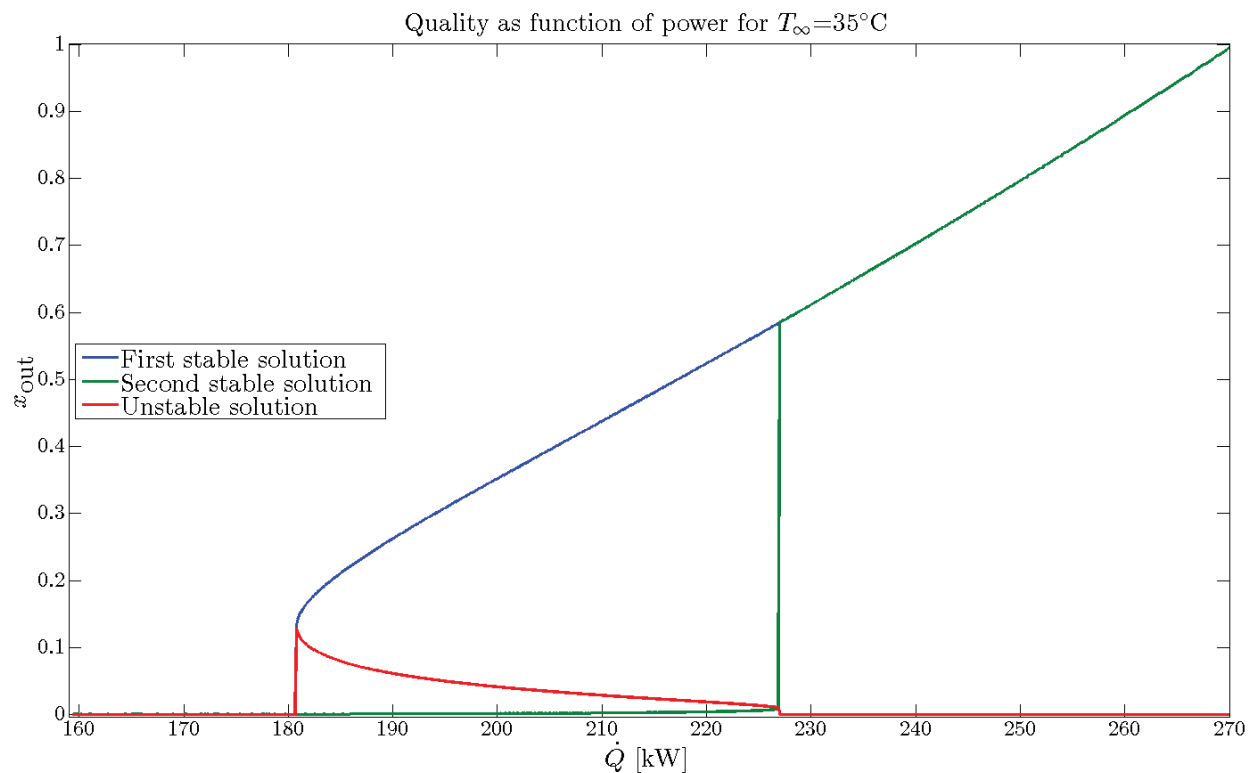


**Figure 5. Quality at channel exit for different powers at full pool inventory for high subcooling.**

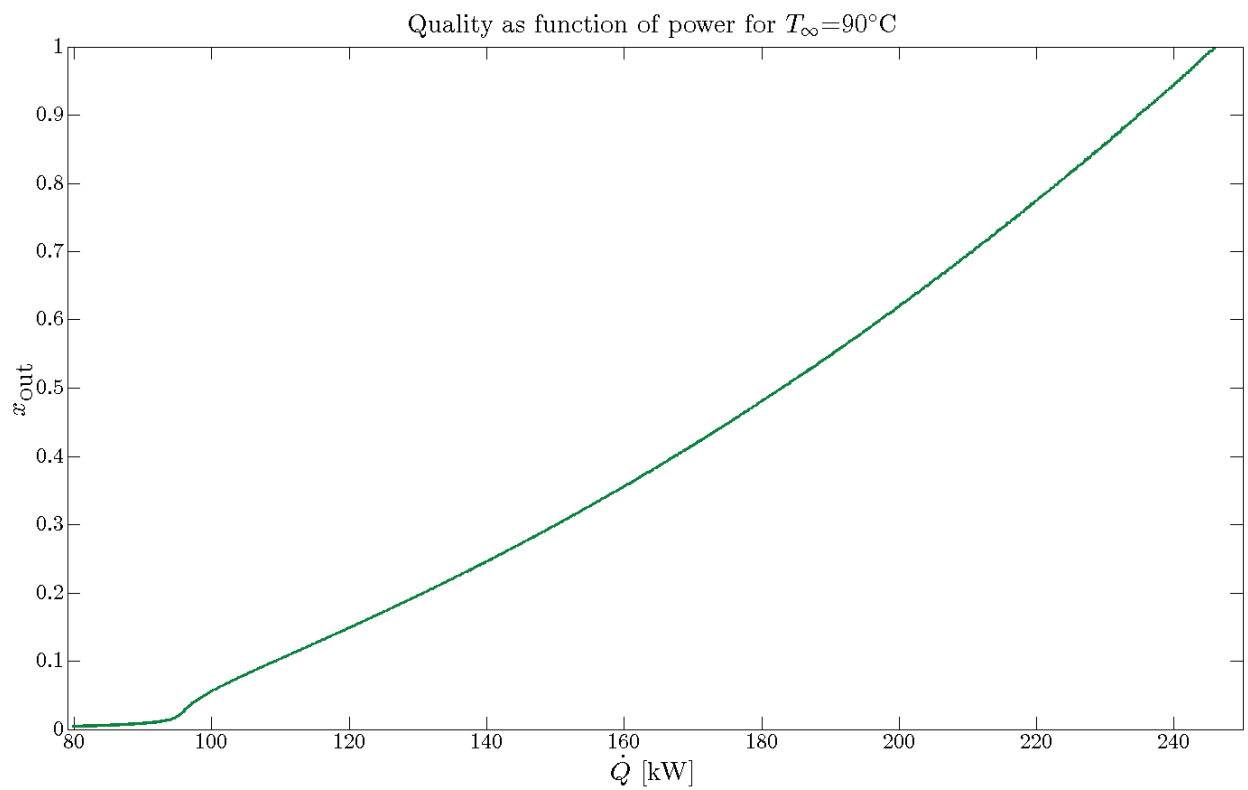


**Figure 6. Quality at channel exit for different powers at full pool inventory for low subcooling.**

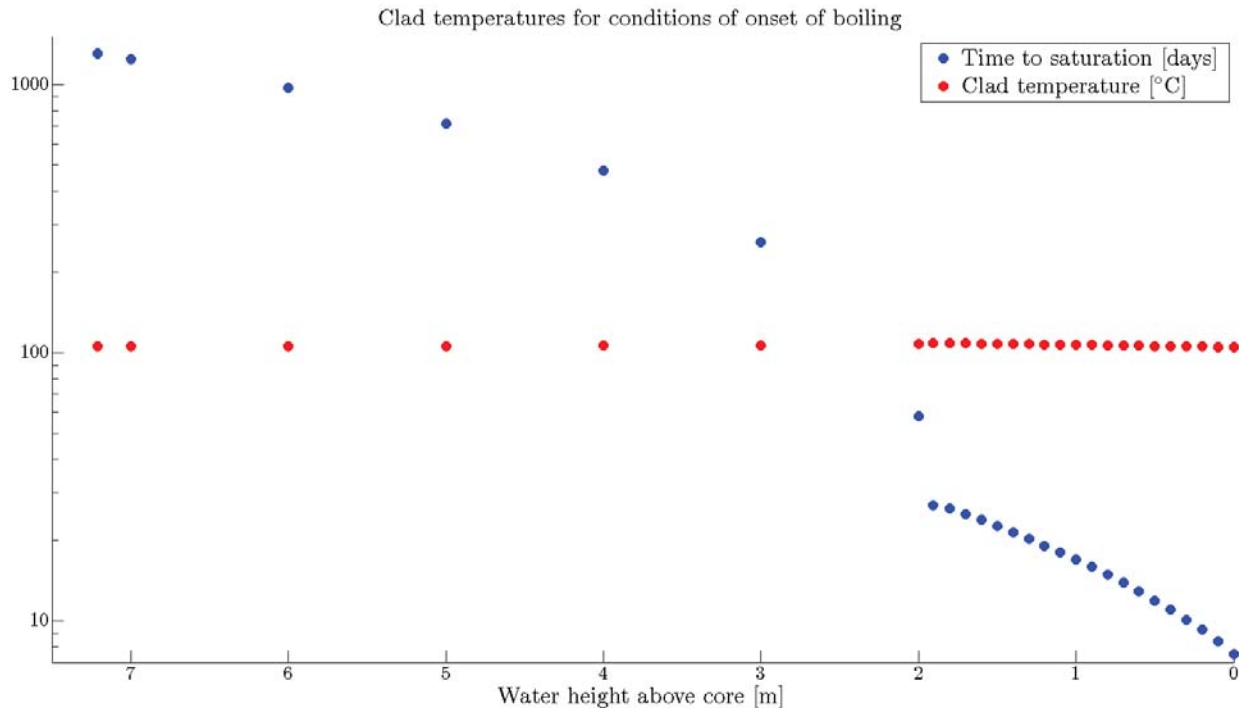


**Figure 7. Times to reach saturation at the exit of the hottest channel for pool draining events and the corresponding temperatures right after initiation of boiling at these times (two-phase model)**

#### 4. CONCLUSIONS

A NC model for a PWR closed loop using the 1-D momentum equation was modified for use in an open pool MTR. The NC model calculates the steady state flow rate and flow quality (if there is boiling) along a fuel assembly given the inlet liquid temperature and assembly power, thus allowing to calculate the fuel and clad temperatures along the channel. The model can be incorporated into models for evaluating open pool temperature and inventory evolution as has been shown by using a simplistic conservative pool heat up model. This may also be useful for safety assessment of spent fuel pool storages, given necessary adjustments.

This model was used to perform a safety evaluation of decay heat removal in the MNR pool for different draining and heat up scenarios. It is shown that for all scenarios before core uncover, clad and fuel temperatures remain far below limiting values. In the worst case examined, where draining is halted just before core uncover, the operators have about 7 days to intervene before any boiling starts in the core.

#### REFERENCES

1. Y. Zvirin, “A Review of Natural Circulation Loops in Pressurized Water Reactors and Other Systems”, *Nuclear Engineering and Design* **67**(2), pp. 203–225 (1982).
2. R. Greif, “Natural Circulation Loops”, *Journal of Heat Transfer* **110**(4b), pp. 1243–1258 (1988).
3. N. E. Todreas and M. S. Kazimi, *Nuclear systems II: Elements of Thermal Hydraulic Design*. Chapter 3, Taylor & Francis, FL, USA (1990).

4. W.R. Gambill and R.D. Bundy, "Heat-Transfer Studies of Water Flow in Thin Rectangular Channels. Part II. Boiling Burnout Heat Flux for Low-Pressure Water in Natural Circulation", *Nuclear Science and Engineering (US)* **18** (1964).
5. Y. Zvirin, A. Shitzer, and G. Grossman, "The Natural Circulation Solar Heater-Models with Linear and Nonlinear Temperature Distributions", *International Journal of Heat and Mass Transfer* **20**(9), pp. 997–99 (1977).
6. B. R. Munson, D. F. Young, and T. H. Okiishi, *Fundamentals of Fluid Mechanics*, John Wiley & Sons, NY, USA (1990).
7. M. M. El-Wakil, *Nuclear Heat Transport*, American Nuclear Society, Michigan, USA (1978).
8. F. P. Incropera, D. P. Dewitt, T. L. Bergman, and A. S. Lavine, *Introduction to Heat Transfer*, John Wiley & Sons, USA (2011).
9. F. P. Incropera, D. P. Dewitt, T. L. Bergman, and A. S. Lavine, *Fundamentals of Heat and Mass Transfer*, John Wiley & Sons, USA (2011).
10. S. G. Kandlikar, "A General Correlation for Saturated Two-Phase Flow Boiling Heat Transfer Inside Horizontal and Vertical Tubes", *Journal of Heat Transfer* **112**(1), pp. 219–228 (1990).

## NOMENCLATURE

$A_i$  = cross sectional area for coolant flow of assembly section denoted by number  $i$

$A_{\text{pool}}$  = pool's surface area,  $\text{m}^2$

$\bar{c}_p$  = average specific heat between two temperatures,  $\text{kJ kg}^{-1} \text{K}^{-1}$

$D$  = hydraulic diameter, m

$f$  = friction factor, unitless

$g$  = gravitational acceleration const,  $\text{m s}^{-2}$

$G$  = mass flux,  $\text{kg m}^{-2} \text{s}^{-1}$

$h_{\text{fg}}$  = latent heat of vaporization,  $\text{kJ kg}^{-1}$

$h$  = heat transfer coefficient,  $\text{W K}^{-1} \text{m}^{-2}$

$\Delta H$  = decrease in pool height, m

$K$  = minor/form/geometry loss coefficient, unitless

$L$  = lengths of assembly sections

$k$  = thermal conductivity,  $\text{W K}^{-1} \text{m}$

$L_{1\phi}$  = length of heated channel occupied by single-phase liquid

$L_{2\phi}$  = length of heated channel occupied by two-phase mixture

$\dot{M}$  = mass flow rate through the assembly,  $\text{kg s}^{-1}$

$M_{\infty}$  = mass of pool inventory, kg

$\rho_g$  = saturated vapor density

$\Delta p_b = -\phi \rho g dl$ , hydrostatic buoyancy term

$\phi^2$  = two-phase multiplier, unitless

$\Delta p_f = \phi f \frac{G|G|}{2D\rho} dl$ , pressure loss term

### Subscripts

b = buoyancy

c = clad

f = friction

fm = fuel meat

out = denoting properties at assembly exit

w = water

$\infty$  = denoting pool and assembly inlet properties

### Abbreviations

CHF = Critical Heat Flux

MNR = McMaster Nuclear Reactor

MTR = Material Testing Reactor

NC = Natural Convection

PWR = Pressurized Water Reactor

1-D = one dimensional